EurJIC
European Journal of Inorganic Chemistry

Full Papers
doi.org/10.1002/ejic.202100419

Chemistry Europe
European Chemical Societies Publishing

Very Important Paper

NMR-Spectroscopic Detection of an Elusive Protonated and Coinage Metalated Silicide $[NHC^{Dipp}Cu(\eta^4\text{-}Si_9)H]^{2-}$ in Solution

Verena Streitferdt+,[a] Susanne M. Tiefenthaler+,[b] Ilya G. Shenderovich,[c] Stefanie Gärtner,[c] Nikolaus Korber,*[b] and Ruth M. Gschwind*[a]

A simultaneously protonated and functionalized silicide cluster $[NHC^{Dipp}Cu(\eta^4\text{-}Si_9)H]^{2-}$ was detected and characterized in liquid ammonia by NMR spectroscopy. Key NMR results were corroborated by theoretical calculations. ^{1}H-NMR line-widths at variable temperatures revealed that proton hopping in the metalated complex $[NHC^{Dipp}Cu(\eta^4\text{-}Si_9)H]^{2-}$ is less pronounced than in the non-complexed silicide $[HSi_9]^{3-}$. Besides $[HSi_9]^{3-}$ and $[NHC^{Dipp}Cu(\eta^4\text{-}Si_9)H]^{2-}$ also the unprotonated analogous cluster $[NHC^{Dipp}Cu(\eta^4\text{-}Si_9)]^{3-}$ was detected in solution. In addition, a new ^{29}Si-NMR signal was obtained in the course of ^{29}Si-NMR studies that we assigned to $[NHC^{Dipp}Cu(\eta^4\text{-}Si_9)]^{3-}$. The isolation of crystals of $(K[2.2.2]\text{-crypt})_2K_{0.48}Rb_{3.52}[NHC^{Dipp}Cu(\eta^4\text{-}Si_9)]_2$ prove the availability of the non-protonated $NHC^{Dipp}Cu(\eta^4\text{-}Si_9)$ fragment in solution. To the best of our knowledge the detection of $[NHC^{Dipp}Cu(\eta^4\text{-}Si_9)H]^{2-}$ represents the first case of a protonated and coinage metalated group 14 *Zintl* cluster in solution so far.

Introduction

Silicon holds an important role in our daily lives, as the use of Si-based technology is now, more than ever, ubiquitous. The semiconducting property of silicon renders it a useful material for nanoelectronics. Over the last years, the polyanionic clusters (*Zintl* ions) of silicon have garnered interest in the fields of mesostructured extended solids, new crystalline modifications and nanoparticles,[1] since they constitute preformed, soluble building blocks. Especially functionalized silicon-building blocks have proven to be useful, as their functionalization enables control of the size of nanoparticles.[2] Only recently, the core expansion of siliconoids by transition metals provided complexes capable of catalytically isomerizing alkenes.[3] However, not just functionalized, but also protonated silicon compounds are of interest in terms of hydrogen-doped amorphous silicon as a promising material for solar cells.[4] Group 14 *Zintl* ions can be functionalized and modified by silylation, transition metal complexation or oxidative coupling reactions.[5–7] While the heavier homologues Ge, Sn and Pb were found to have an extensive coordination chemistry, such as $[Pt@Sn_9Pt(PPh_3)]^{2-}$,[8] $[Pb_9W(CO)_3]^{4-}$,[9] or $\{(Ge_9)_2[\eta^6\text{-}Ge(PdPPh_3)_3]\}^{4-}$,[10] transition metal (TM) functionalized silicides are still rare. So far, only five compounds are known which contain a silicon *Zintl* ion acting as the ligand in a metal complex. Beside the reported complexes $[Si_9ZnPh]^{3-}$ by Sevov *et al.*,[11] as well as $[(MesCu)_2Si_4]^{4-}$ and $[NHC^{Dipp}Cu(\eta^4\text{-}Si_9)]^{3-}$ (the latter was experimentally characterized by crystal structure, ESI-MS and ^{1}H-NMR) by Fässler *et al.*,[12,13] we were able to synthesize and characterize $[\{Ni(CO)_2\}_2(\mu\text{-}Si_9)_2]^{8-}$ and more recently $[(NHC^{tBu}Au)_6(\eta^2\text{-}Si_4)]^{2+}$.[14,15]

Zintl ions and their functionalized analogues are mainly characterized *via* single crystal X-ray diffraction. However, Rudolph *et al.* already demonstrated that especially solution NMR can provide valuable information about structures, solution-equilibria or dynamics. They used ^{119}Sn-NMR to experimentally prove the fluctuation of the nonastannide[16] Sn_9^{4-} that had already been postulated by Corbett *et al.* the year before.[17] Subsequently, more and more results were obtained *via* ^{119}Sn-and ^{207}Pb-NMR,[18] as well as more recently *via* ^{29}Si-NMR.[19] The groups of Eichhorn[20] and Schrobilgen[9] were the first to report on NMR signals stemming from a TM functionalized stannide, when they both discovered the three distinct resonances of the compound $M(CO)_3Sn_9$ (M = Cr, Mo, W) in the ^{119}Sn-NMR. Since then a number of *Zintl* ions other than silicides with exo-bound metal complexes have been detected and reported on.[18] In addition, Eichhorn *et al.* were able to obtain

---

[a] Dr. V. Streitferdt,+ Prof. Dr. R. M. Gschwind
Institute of Organic Chemistry
University of Regensburg
93040 Regensburg, Germany
E-mail: Ruth.Gschwind@ur.de
http://www-oc.chemie.uni-regensburg.de/gschwind/

[b] S. M. Tiefenthaler,+ Prof. Dr. N. Korber
Institute of Inorganic Chemistry
University of Regensburg
93040 Regensburg, Germany
E-mail: Nikolaus.Korber@ur.de
https://www.uni-regensburg.de/chemie-pharmazie/anorganische-chemie-korber/startseite/index.html

[c] Dr. I. G. Shenderovich, Dr. S. Gärtner
Central Analytics
University of Regensburg
93040 Regensburg, Germany
https://www.uni-regensburg.de/chemie-pharmazie/zentrale-analytik/startseite/index.html

[+] These authors contributed equally.

Supporting information for this article is available on the WWW under https://doi.org/10.1002/ejic.202100419 the first NMR signals of some endohedral *Zintl* cages $[M@Pb_{12}]^{2-}$ (M = Pt, Pd, Ni),[21] which were followed by reports on NMR signals of clusters such as $[Pd_2@Sn_{18}]^{4-}$ by Wang *et al.*[22] or $[Cu@Sn_9]^{3-}$ by Fässler *et al.*[23]

Compared to the rich chemistry of *Zintl* ions of tin and lead, little is known about silicides, especially about their structures in solution *via* NMR studies, as opposed to siliconoids, which have been extensively studied in their unsaturated[24] and recently also TM-functionalized form.[25] There are many reasons for this, e.g. the difficulties in synthesizing, handling and preparing the silicide samples as well as the low solubility in ammonia combined with the low natural abundance of the NMR active ^{29}Si. These factors, together with the long relaxation time of ^{29}Si, lead to low signal to noise ratios, making the recording and evaluation of spectra difficult and time consuming.

Recently, reports of the protonated silicon *Zintl* ions $[HSi_9]^{3-}$, $[H_2Si_9]^{2-}$ and $[HSi_4]^{3-}$ in solution have been published,[26–28] relying on NMR studies as well as on crystal structures.[29] Whereas Eichhorn *et al.* have previously only reported on rapid intramolecular proton scrambling in the compound $[HSn_9]^{3-}$,[30] our study on $[HSi_9]^{3-}$ revealed a fluxional behavior of the Si–H and more unexpectedly of the Si–Si bonding.[26] Shortly after that, we reported on our findings of the cluster $[HSi_4]^{3-}$ which demonstrated the importance of charge delocalization upon protonation of silicides.[28] In addition, solution studies can provide valuable information about chemical exchange processes and discrepancies between observed structures in solution and solid state.[15,20,31]

Simultaneously protonated and TM functionalized *Zintl* clusters are rare and mainly known for the heavier homologues Ge and Sn ($[(\mu_2\text{-H})(\eta^2\text{-Ge}_4)ZnPh_2]^{3-}$ or $[M@Sn_9H]^{3-}$ with M = Pt, Pd, Ni).[32,33] In contrast, for silicides such a protonated and TM functionalized complex is still elusive in crystals and in solution. So far, only in the gas phase ESI-MS indicated the existence of a $\{[(NHC^{Dipp}Cu)_n(Si_9)]^{(4-n)-} + (3-n)H^+\}^-$ with n = 1, 2.[13]

To fill this gap, we here report the detection of a protonated and TM functionalized silicon cluster $[NHC^{Dipp}Cu(\eta^4\text{-Si}_9)H]^{2-}$ in solution which is further supported by crystallographic and computational analyses. To the best of our knowledge, this also represents the first case of a protonated coinage metalated group 14 *Zintl* cluster detected in solution. In addition, we report on elusive ^{29}Si-NMR shifts of the analogous unprotonated cluster $[NHC^{Dipp}Cu(\eta^4\text{-Si}_9)]^{3-}$ generated in situ in the NMR tube.

Results and Discussion

NMR Spectroscopic Studies

For the NMR studies, samples of the *Zintl* phase $K_6Rb_6Si_{17}$ (fully ^{29}Si enriched) in the presence of NHC^{Dipp}CuCl (2 eq.) and [2.2.2]-cryptand (2 eq.) in liquid ammonia were prepared. Sample preparation, handling and investigation of such samples by NMR are not trivial. The low solubility of the *Zintl* phase and the presence of quadrupolar nuclei (^{63}Cu/^{65}Cu) entail signal-to-noise (S/N) problems and pose a challenge even for standard 1D experiments. This together with signal overlap also renders integration an intricate task. The dissolution and transformation process of NHC^{Dipp}-containing species was followed by ^{1}H-NMR (see Figure S1 in the Supporting Information). After 28 days well resolved multiplets were observed in (i) the region characteristic for unsaturated NHC^{Dipp}-protons and (ii) the chemical shift region typical for protonated silicides (see Figure 1a). The signals depicted in Figure 1 could be assigned to three different silicon *Zintl* clusters through various 1D and 2D ^{1}H- and ^{29}Si-NMR experiments. These clusters are the $[HSi_9]^{3-}$ and the $[NHC^{Dipp}Cu(\eta^4\text{-Si}_9)]^{3-}$ (**1**), both known in literature,[13,26,29] and the $[NHC^{Dipp}Cu(\eta^4\text{-Si}_9)H]^{2-}$ (**2**), a protonated coinage metalated group 14 *Zintl* cluster detected in solution (for structures see Figure 1). The $[HSi_9]^{3-}$ could unambiguously be assigned to the characteristic doublet at $\delta(^1\text{H at 233 K}) = -1.88$ ppm with $^1J_{HSi} = 156$ Hz via 2D ^{1}H-^{29}Si-HMQC experiments (see Figure S6 in the Supporting Information). The structural characterization of **1** and its protonated analogue **2** will be discussed in detail in the following.

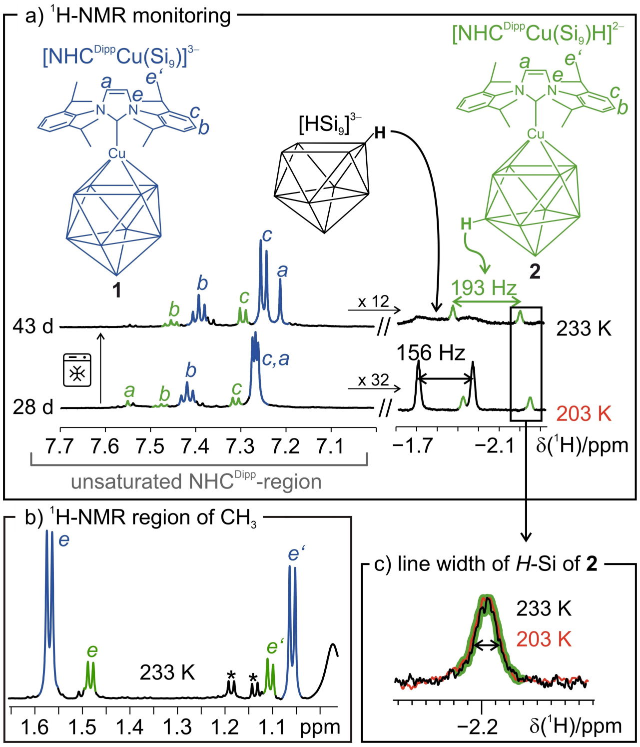

Figure 1. ^{1}H-NMR detection of $[NHC^{Dipp}Cu(\eta^4\text{-Si}_9)]^{3-}$ (**1**) (blue), $[NHC^{Dipp}Cu(\eta^4\text{-Si}_9)H]^{2-}$ (**2**) (green) and HSi_9^{3-} (black). (a) Reaction process of NHC^{Dipp}CuCl (2 eq.) with $K_6Rb_6Si_{17}$ (fully ^{29}Si enriched) and [2.2.2]-cryptand (2 eq.) in liquid ammonia after 28 d (bottom spectrum) and 43 d (top spectrum). The green high field doublet ($^1J_{HSi} = 193$ Hz) characteristic for protonated silicides in combination with the new set of NHC^{Dipp}-signals indicate the presence of **2** (for details see text). (b) Demonstration of the shift inequality of the CH_3 protons of **1** and **2**. (c) The linewidth of the H–Si signal of **2** stays unaffected upon temperature change indicating a more rigid H-Si_9 cluster in **2** than in pure HSi_9^{3-}. For time between preparation and NMR measurement see left, for temperature see right. After 21 h, the NMR tube was shaken to facilitate the dissolution of silicides. The freezer symbol indicates storage of the sample at 193 K. For the sake of clarity, the H–Si region (28 d and 43 d) was scaled (×32 and ×12 respectively). The spectral regions in (c) are shifted and intensity adapted to enable a direct linewidth comparison.

Characterization of $[\mathrm{NHC}^{\mathrm{Dipp}}\mathrm{Cu}(\eta^4\text{-}\mathrm{Si}_9)]^{3-}$ (1)

The different spin systems of the major set of the $\mathrm{NHC}^{\mathrm{Dipp}}$-characteristic ^{1}H-NMR signals (marked in blue in Figure 1a) were assigned to the same species via integration, ^{1}H-^{1}H-COSY, -NOESY, ^{1}H-^{13}C-HSQC and -HMBC experiments (for spectra and further information see text and Figure S2, S3 and S4 in the Supporting Information). The CH_3 protons of this ligand set exhibit considerable shift inequality (see Figure 1b) which is commonly observed for $\mathrm{NHC}^{\mathrm{Dipp}}$Cu moieties connected to *Zintl* ions.[34–36] These ^{1}H-NMR shifts and the characteristic shift inequality of the CH_3 groups fit very well to the previously reported[13] metalated cluster **1** (see Figure 1b) and were therefore assigned to **1**. In addition, in a long-term investigation of the sample, a ^{29}Si-NMR signal at −276 ppm could be detected (probably due to higher S/N associated with full enrichment of ^{29}Si compared to ^{29}Si at natural abundance) that most probably belongs to the Si-cluster of **1** (for a more detailed discussion of this signal see the Supporting Information).

Characterization of $[\mathrm{NHC}^{\mathrm{Dipp}}\mathrm{Cu}(\eta^4\text{-}\mathrm{Si}_9)\mathrm{H}]^{2-}$ (2)

The less prominent set of $\mathrm{NHC}^{\mathrm{Dipp}}$-characteristic ^{1}H-NMR signals (marked in green in Figure 1a) was found to correlate in signal increase and decrease behavior over time with a doublet at $\delta(^1\mathrm{H}\text{ at }233\text{ K}) = -2.04$ ppm suggesting a structural affiliation (for full spectra see Figure S3 in the Supporting Information). This doublet has neither been observed in any of our previous NMR investigations of *Zintl* phases nor, to the best of our knowledge, has it been reported in literature so far. Its negative ^{1}H-NMR chemical shift is indicative of an attachment to a polyatomic silicide cluster (compare with $[\mathrm{HSi}_9]^{3-}$ $\delta(^1\mathrm{H}) = -2.85$ ppm;[26] $[\mu\text{-}\mathrm{HSi}_4]^{3-}$ $\delta(^1\mathrm{H}) = -10.62$ ppm;[28] $[\mathrm{H}_2\mathrm{Si}_9]^{2-}$ $\delta(^1\mathrm{H}) = -0.71$ ppm[27]).[37] The hydrogen silicon bond and its $^1J_{\mathrm{HSi}}$ could be confirmed by the observed cross peak in 2D ^{1}H-^{29}Si-HMQC spectra and by 1D ^{1}H{^{29}Si}-NMR spectra with selective silicon decoupling (see Figure 2 and Figure S3) revealing the attachment of this hydrogen to a silicon at −135 ppm.[38] Further information about the protonation of this cluster could be drawn from the green signal at −2.04 ppm: (i) the doublet splitting pattern indicates that the silicide is protonated at a vertex, not an edge; (ii) the large coupling constant of 193 Hz implies that only one hydrogen is attached (compare $[\mathrm{HSi}_9]^{3-}$ $^1J_{\mathrm{HSi}} = 156$ Hz[26] in contrast to $[\mathrm{H}_2\mathrm{Si}_9]^{2-}$ $^1J_{\mathrm{HSi}} = 19.7$ Hz[27]). In addition, the correlation of the doublet at −2.04 ppm with a set of $\mathrm{NHC}^{\mathrm{Dipp}}$ ^{1}H-NMR signals suggests simultaneous functionalization of this silicide cluster by an $\mathrm{NHC}^{\mathrm{Dipp}}$Cu fragment (see above). This is corroborated by the CH_3 protons of the green ligand set which exhibits considerable shift inequality (for spectra see Figure S1) similar to the CH_3 protons[13] of $[\mathrm{NHC}^{\mathrm{Dipp}}\mathrm{Cu}(\eta^4\text{-}\mathrm{Si}_9)]^{3-}$. This together with the integral ratios of $\mathrm{NHC}^{\mathrm{Dipp}}$: H-Si = 1 : 1 unveils that the green signals in Figure 1a correspond to a mono-protonated silicide attached to one $\mathrm{NHC}^{\mathrm{Dipp}}$Cu unit. Next, the cluster size of this protonated and transition metal functionalized silicide (Si_x^{y-}) was addressed. Since the applied *Zintl* phase $\mathrm{K}_6\mathrm{Rb}_6\mathrm{Si}_{17}$ consists of preshaped Si_9^{4-} and Si_4^{4-} clusters, an Si_9- or Si_4-unit seemed most obvious as core structure (an Si_5-unit was excluded since protonation of this cluster was calculated to be highly unfavored[28]). In particular, an Si_9-unit was considered more likely than Si_4. On the one hand, ^{1}H- and ^{29}Si-NMR shifts of this protonated and functionalized cluster are close to those reported for the $[\mathrm{HSi}_9]^{3-}$. On the other hand, Si_9-containing clusters **1** and $[\mathrm{HSi}_9]^{3-}$ were detected as the main derivatized silicide species in solution[39] and **1** was the only cluster found in corresponding crystallization experiments. All in all, we propose the green structure depicted in Figure 1 for this protonated and transition metal functionalized cluster $[\mathrm{NHC}^{\mathrm{Dipp}}\mathrm{Cu}(\eta^4\text{-}\mathrm{Si}_9)\mathrm{H}]^{2-}$ (**2**). Despite all efforts, we were not able to detect any further correlation of the silicide bound hydrogen to other silicon atoms than the directly bound silicon of the cluster via 2D ^{1}H-^{29}Si-HMQC. However, this is not taken as an exclusion criterion for the presence of a polyatomic Si-cluster since low S/N ratios, line broadening induced by interactions with the quadrupole Cu and the reduced cluster flexibility expected upon metalation (as in the case of $\mathrm{E}_9\mathrm{M(CO)}_3$ with E = Sn, Pb; M = Cr, Mo, W)[9,20] probably impede the detection of further H–Si correlations. A reduced flexibility of **2** compared to $[\mathrm{HSi}_9]^{3-}$ was indicated by ^{1}H-NMR spectra recorded at different temperatures (203 K and 233 K). Upon temperature increase the line width of the H–Si signal of **2** remained unaltered (see Figure 1a and Figure 1c) in contrast to that of $[\mathrm{HSi}_9]^{3-}$, in which H-hopping[26] leads to a severe line broadening (see Figure 1a). The reduced flexibility of **2** is in line with observations of Eichhorn *et al.*[20] and Schrobilgen *et al.*[9] that the flexibility for *Zintl* complexes

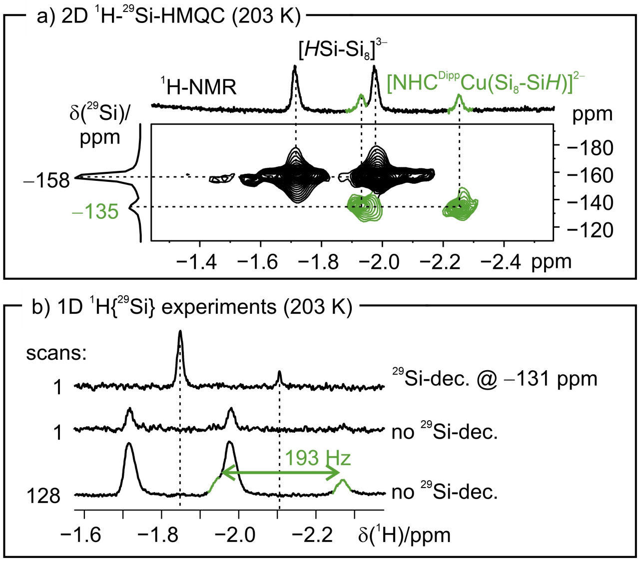

Figure 2. 2D ^{1}H-^{29}Si-HMQC spectra and 1D ^{1}H{^{29}Si}-NMR spectra unveil the attachment of the hydrogen assigned to $[\mathrm{NHC}^{\mathrm{Dipp}}\mathrm{Cu}(\eta^4\text{-}\mathrm{Si}_9)\mathrm{H}]^{2-}$ (**2**) to a silicon signal at $\delta(^{29}\mathrm{Si}) = -135$ ppm. (a) Slice of a 2D ^{1}H-^{29}Si-HMQC spectrum recorded 31 days after sample preparation at 203 K. (b) ^{1}H{^{29}Si}-NMR decoupling experiments recorded 44 days after sample preparation at 203 K revealed that the splitting of 193 Hz of the signal at $\delta(^1\mathrm{H}) = -2.1$ ppm is caused by coupling to the silicon signal at $\delta(^{29}\mathrm{Si}) = -135$ ppm. For more information on (a) and (b) see Figure S6.

($E_9M(CO)_3$ with E = Sn, Pb; M = Cr, Mo, W) decreases upon metalation.[40] Against this experimental background, theoretical calculations were performed to verify the structure of this cluster (see below).

Theoretical Calculations to Validate the Structure of 2

Calculations at the ωb97xd/def2tzvp[41,42] level of theory using the solvation model based on density (SMD[43]) were performed to check for structural energetic minima and to validate the experimental NMR data. This functional/basis combination reproduces chemical shifts with an accuracy of better than ± 9 ppm.[44] However, NMR chemical shifts and coupling constants depend on non-covalent interactions and the electric field generated by the surrounding.[45,46] The magnitude of the corresponding changes depends not so much on the type of nucleus as on the specific molecular structure, and cannot always be accurately reproduced using the simplified SMD approach.[47] For example, for $[HSi_9]^{3-}$ the difference between the experimental and calculated values was small for chemical shifts and large for $^1J_{\mathrm{HSi}}$.[26] For $[HSi_4]^{3-}$ this difference in ^{29}Si NMR chemical shifts was from 60 to 80 ppm, while very small for $^1J_{\mathrm{HSi}}$ and $^1J_{\mathrm{SiSi}}$.[28] Of course, all of the above applies to the energy of the structure in question.

For two complex structures **A** and **B** energetic minima were found for hydrogens located at vertices (see Figure 3). A corresponding complex with a bridging hydrogen bound to silicon atoms in the Cu-Si_4 unit was found to be very energetically disfavored (see Figure S15). Complex **A** is energetically slightly favored over **B** by 9 kJ/mol, in contrast calculated ^{1}H- and ^{29}-Si NMR chemical shifts are in better accordance with complex **B**. Overall, we rank the better agreement of **B** with chemical shifts higher than the small energetic preference of **A** and therefore consider **B** as the better structural model for **2**.[48]

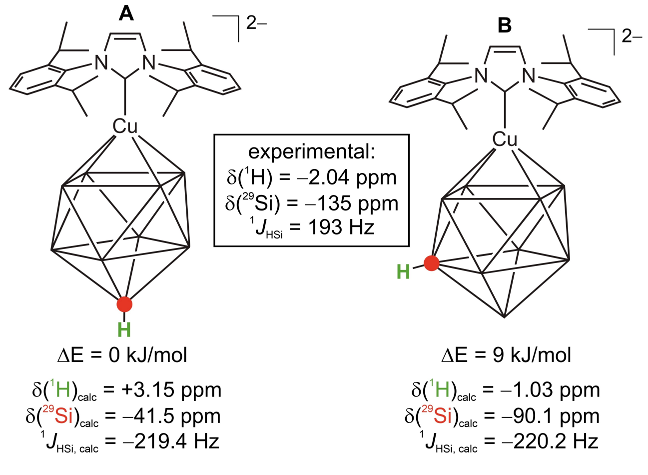

Figure 3. Calculated lowest energetic complex structures **A** and **B** of $[\mathrm{NHC^{Dipp}Cu}(\eta^4\text{-}Si_9)H]^{2-}$ (**2**). Complex **A** is energetically slightly favored over **B** while calculated ^{1}H- and ^{29}Si-NMR chemical shifts are in better accordance with complex **B**.

The comparison of calculated and experimental $^1J_{\mathrm{HSi}}$ of **2** and $[HSi_9]^{3-}$ ($^1J_{\mathrm{HSi,\ calc.}}$ = 189 Hz; $^1J_{\mathrm{HSi,\ exp.}}$ = 156 Hz)[26] provides additional information. The experimental value of **2** is smaller than the calculated one analogous to the case of $[HSi_9]^{3-}$. For $[HSi_9]^{3-}$ the reason for the reduced experimental coupling constant is assumed to be a result of proton hopping. Hence, the reduced experimental $^1J_{\mathrm{HSi}}$ of **2** also presumably indicates a certain extent of proton hopping. Thus, in **2** proton hopping is most likely present, yet less pronounced than in $[HSi_9]^{3-}$. The latter is consistent with the ^{1}H-line shape analysis (see above and Figure 1).

Crystallization Study

For the crystallization study, a solution of a phase with the nominal composition $K_6Rb_6Si_{17}$, $\mathrm{NHC^{Dipp}CuCl}$ and [2.2.2]-cryptand in liquid ammonia was prepared. After three months of storage at 233 K, yellow crystals of $(K[2.2.2]\text{-crypt})_2K_{0.48}Rb_{3.52}[\mathrm{NHC^{Dipp}Cu}(\eta^4\text{-}Si_9)]_2 \cdot 15.2\ NH_3$ **1** were isolated[49] and measured under constant cooling. While the central moiety $[\mathrm{NHC^{Dipp}Cu}(\eta_4\text{-}Si_9)]^{3-}$ is known from the structure $A_3[A[2.2.2]\text{-crypt}]_3[\mathrm{NHC^{Dipp}Cu}(\eta^4\text{-}Si_9)]_2 \cdot 26\ NH_3$ (A = K, K/Rb, Rb) published by Fässler *et al.* in 2017, the cationic counterpart is different. In addition to the two complexed potassium atoms in the [2.2.2]-crypt, four cation positions are present in the structure. The central moiety of the compound consists of a chain of $[\mathrm{NHC^{Dipp}Cu}(\eta^4\text{-}Si_9)]^{3-}$ cages connected *via* rubidium atoms along the crystallographic *b*-axis. Two of these chains are further connected *via* two alkali metal positions along the crystallographic *a*-axis, leading to double strands along *b* (see Figure S10–12). The formation of these double strands is in contrast to the single strands observed in $A_3[A[2.2.2]\text{-crypt}]_3[\mathrm{NHC^{Dipp}Cu}(\eta^4\text{-}Si_9)]_2 \cdot 26\ NH_3$ (A = K, K/Rb, Rb). All distances are in similar ranges as the distances reported for the compound $A_3[A[2.2.2]\text{-crypt}]_3[\mathrm{NHC^{Dipp}Cu}(\eta^4\text{-}Si_9)]_2 \cdot 26\ NH_3$, with the Cu–Si distances between 2.4174(14) and 2.4786(13) Å and the Si–Si distances between 2.4038(18) and 2.653(2) Å. Further details of the crystal structure investigation can be obtained from the FIZ Karlsruhe by quoting the deposition number CSD-2043546.

A comprehensive overview of ^{29}Si NMR shifts of silicon *Zintl* anions in solution reported in literature is provided in Figure 4.

Conclusion

In summary, characteristic signals of a simultaneously protonated and functionalized silicide cluster could be detected in solution by NMR spectroscopy. Their assignment to $[\mathrm{NHC^{Dipp}Cu}(\eta^4\text{-}Si_9)H]^{2-}$ (**2**) was supported *via* NMR by signal monitoring, integration and 2D experiments and *via* theoretical calculations. In addition, NMR revealed that the proton hopping in the metalated complex $[\mathrm{NHC^{Dipp}Cu}(\eta^4\text{-}Si_9)H]^{2-}$ is less pronounced than in the non-complexed silicide $[HSi_9]^{3-}$. Furthermore, a ^{29}Si-NMR signal was detected, which most probably belongs to $[\mathrm{NHC^{Dipp}Cu}(\eta^4\text{-}Si_9)]^{3-}$ (**1**). The isolation of crystals of $(K[2.2.2]\text{-crypt})_2K_{0.48}Rb_{3.52}[\mathrm{NHC^{Dipp}Cu}(\eta^4\text{-}Si_9)]_2$ prove the availability of the

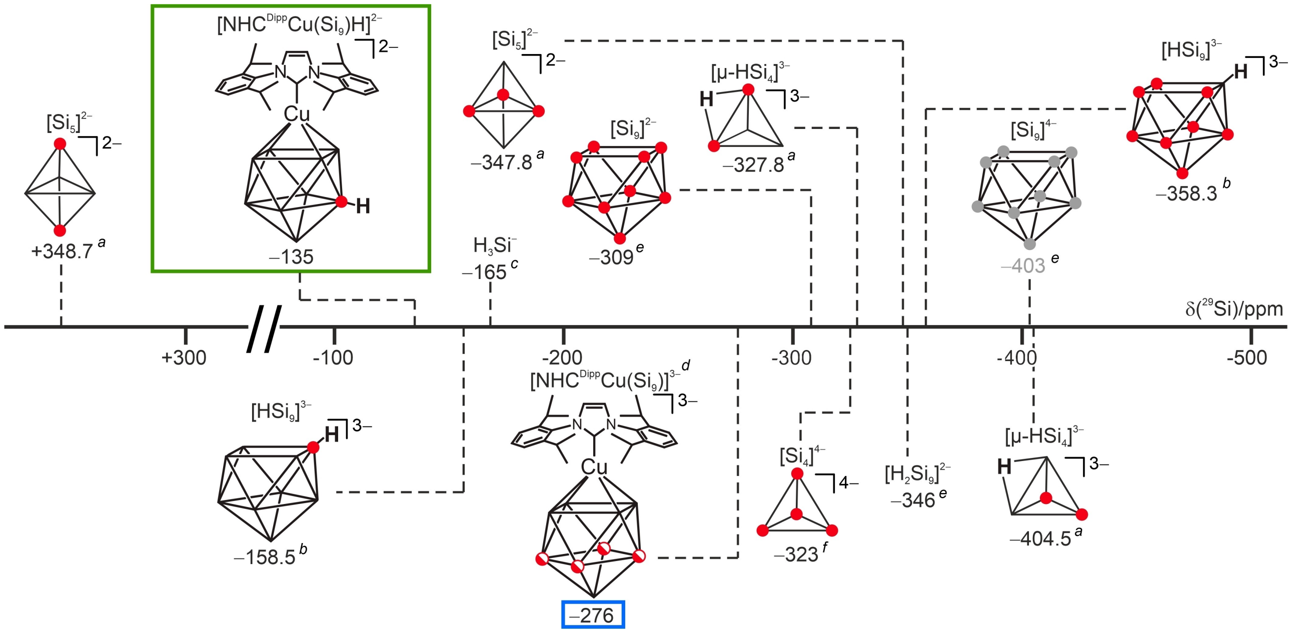

Figure 4. Comprehensive overview of the ^{29}Si-NMR chemical shift range of silicon *Zintl* ions in solution. ^{29}Si-NMR shifts are given for the highlighted silicon atoms. Red indicates experimental shifts, gray calculated shifts. The half-filled balls indicate a tentative assignment. The structure highlighted in green ($[NHC^{Dipp}Cu(\eta^4\text{-}Si_9)H]^{2-}$) was detected and investigated in this study by NMR and theoretical calculations. A hitherto unknown ^{29}Si-NMR signal of $[NHC^{Dipp}Cu(\eta^4\text{-}Si_9)]^{3-}$ with the shift highlighted in blue could be detected in this work. Shifts taken from literature: *a*,[28] *b*,[26] *c*,[50] *e*,[27] *f*.[15] Literature *d*[13] provides experimental characterization of $[NHC^{Dipp}Cu(\eta^4\text{-}Si_9)]^{3-}$ by crystal structure, ESI-MS and ^{1}H-NMR but not by ^{29}Si-NMR.

non-protonated $NHC^{Dipp}Cu(\eta^4\text{-}Si_9)$ fragment in solution. To our knowledge, the detection of $[NHC^{Dipp}Cu(\eta^4\text{-}Si_9)H]^{2-}$ represents the first case of a protonated, coinage metalated group 14 *Zintl* cluster in solution so far.

Experimental Section

Crystallization Study

All operations were carried out under argon atmosphere, either in a glovebox or with the help of Schlenk techniques. Liquid ammonia was dried and stored over sodium and cooled with a dry ice/ethanol mixture. Rubidium was synthesized by reduction of RbCl with calcium and subsequently purified by distillation.[51]

Synthesis of $K_6Rb_6{}^{29}Si_{17}$ (99.2% enriched) and $K_6Rb_6Si_{17}$: The compound was synthesized via solid-state reaction techniques. Elemental potassium (119.1 mg, 3.05 mmol), rubidium (260.3 mg, 3.05 mmol) and enriched silicon (250.0 mg, 8.63 mmol) were put into a tantalum ampoule that was subsequently welded shut and jacketed in a fused silica ampoule. The ampoule was heated to 973 K at a rate of 25 K/h, held at that temperature for 24 hours and subsequently cooled to room temperature at 20 K/h. The brittle, black reaction product was isolated and stored in an argon filled glovebox. The same procedure was used in the preparation of $K_6Rb_6Si_{17}$ with non-enriched silicon (974.5 mg, 34.70 mmol), potassium (478.8 mg, 12.25 mmol) and rubidium (1046.7 mg, 12.25 mmol) where the ampoule was heated to 1223 K at a rate of 25 K/h, held at that temperature for 2 hours and subsequently cooled to room temperature at 20 K/h.

Synthesis of $(K[2.2.2]\text{-crypt})_2K_{0.48}Rb_{3.52}[NHC^{Dipp}Cu(\eta^4\text{-}Si_9)]_2\cdot 15.2\ NH_3$ (1): $K_6Rb_6Si_{17}$ (150 mg, 0.12 mmol), $NHC^{Dipp}CuCl$ (59.7 mg, 0.12 mmol) and [2.2.2]-cryptand (69.2 mg, 0.18 mmol) were weighted into a heated Schlenk tube, after which approximately 10 mL of pre-dried ammonia were condensed onto the reactants. The orange-red solution was stored at 193 K for 3 months, before orange crystals of **1** were isolated and characterized via single crystal X-ray diffraction.

X-ray Crystal Structure Determination: In an apparatus similar to the one developed by Kottke and Stalke,[49] perfluorether oil for the crystal selection was cooled in a stream of liquid nitrogen. Crystals were quickly transferred from the cooled reaction vessel into the cooled perfluorether oil under argon counter current. A suitable specimen of the very air- and temperature sensitive crystals was scooped up on a MiTeGen holder and transferred onto the diffractometer in liquid nitrogen. The single crystal data were collected on a SuperNova diffractometer (Agilent), equipped with a molybdenum micro focus X-ray source an EOS CCD-detector. Data reduction was performed using the software CrysAlisPro 41.83a.[52] The software Olex2,[53] as well as the program ShelXT were used for structure solution,[54] ShelXL for the refinement.[55] For visualization Diamond 4 was employed.[56]

Sample preparation for NMR studies: $K_6Rb_6{}^{29}Si_{17}$ (12.5 mg, 0.01 mmol), $NHC^{Dipp}CuCl$ (9.8 mg, 0.02 mmol) and [2.2.2]-cryptand (7.6 mg, 0.02 mmol) were weighed into heated heavy wall precision NMR sample tubes (Pyrex) under an argon atmosphere. Subsequent condensation of ammonia lead to an initially colorless solution, after which the NMR tube was sealed shut by melting under an ammonia atmosphere. The sample was stored at 193 K until examined by NMR.

NMR Studies

NMR spectra were recorded on a Bruker Avance III HD 600 MHz spectrometer equipped with a fluorine selective TBIF probe and a

Bruker Avance NEO 600 MHz spectrometer equipped with a double resonance broad band probe (BBO). ^{1}H-, ^{13}C- (in the Supporting Information) and ^{29}Si-NMR spectra were referenced externally to TMS (tetramethylsilane). ^{1}H-NMR spectra were calibrated on the chemical shift of H_2 (4.60 ppm). In case the ^{29}Si signal of the HSi_9^{3-} was detected, the ^{29}Si-NMR spectra were calibrated on the literature known chemical shift of HSi_9^{3-} (−358.5 ppm). The temperatures 203 K and 233 K were controlled by Bruker BVTE units. Data was processed with the Bruker software TOPSPIN 3.2 and TOPSPIN 4.0.7.

For further information see the Supporting Information.

Computational Details

All geometries were optimized at the ωb97xd/def2tzvp[41,42] level of theory in the continuum of NH_3 (SMD) at 200 K (eps = 22.63; epsinf = 1.76; Rsolv = 1.7; HbondAcidity = 0.14; HbondBasicity = 0.62; SurfaceTensionAtInterface = 29.00; CarbonAromaticity = 0.0; ElectronegativeHalogenicity = 0.0). The dielectric constant was increased to 22.63 to adapt the low temperature measurement. Single point energies was obtained at the MP2/def2qzvpp level of theory on top the optimized geometry.[57] NMR shift and coupling calculations were performed at TPSSH/pcSseg-4.[58] The ^{1}H and ^{29}Si chemical shifts of $[NHC^{Dipp}Cu(\eta^4\text{-}Si_9)H]^{2-}$ were referenced to that of $[HSi_9]^{3-}$.

Deposition Number 2043546 (for $K[2.2.2]crypt)_2K_{0.47}Rb_{3.53}[NHC^{Dipp}Cu(\eta^4\text{-}Si_9)]_2\cdot 15\ NH_3$) contains the supplementary crystallographic data for this paper. These data are provided free of charge by the joint Cambridge Crystallographic Data Centre and Fachinformationszentrum Karlsruhe Access Structures service www.ccdc.cam.ac.uk/structures.

Acknowledgements

We gratefully acknowledge financial support from the German Science Foundation (DFG) (KO 1857/10-1, and GS 13/5-1). Furthermore, we thank Prof. Dr. Burkhard Luy for providing us unpublished xy-BEBOP pulses covering excitation windows of 500 and 1000 kHz respectively. Open access funding enabled and organized by Projekt DEAL.

Conflict of Interest

The authors declare no conflict of interest.

Keywords: Carbene ligands · Copper · Liquid ammonia · Silicides · Structure elucidation · Zintl phases

[1] M. Beekman, S. Kauzlarich, L. Doherty, G. Nolas, *Materials (Basel).* **2019**, *12*, 1139.
[2] M. H. Nayfeh, L. Mitas, *Nanosilicon* (Ed.: V. Kumar), Elsevier Ltd, **2008**, pp. 1–78.
[3] N. E. Poitiers, L. Giarrana, V. Huch, M. Zimmer, D. Scheschkewitz, *Chem. Sci.* **2020**, *11*, 7782–7788.
[4] A. Seyhan, T. Altan, O. C. Ecer, R. Zan, *J. Phys. Conf. Ser.*, Institute Of Physics Publishing, **2017**, p. 12024.
[5] F. S. Geitner, T. F. Fässler, *Inorg. Chem.* **2020**, *59*, 15218–15227.
[6] C. Schenk, A. Schnepf, *Angew. Chem. Int. Ed.* **2007**, *46*, 5314–5316; *Angew. Chem.* **2007**, *119*, 5408–5410.
[7] Y. Wang, J. E. McGrady, Z. M. Sun, *Acc. Chem. Res.* **2021**, *54*, 1506–1516.
[8] B. Kesanli, J. Fettinger, D. R. Gardner, B. Eichhorn, *J. Am. Chem. Soc.* **2002**, *124*, 4779–4786.
[9] J. Campbell, H. P. A. Mercier, H. Franke, D. P. Santry, D. A. Dixon, G. J. Schrobilgen, *Inorg. Chem.* **2002**, *41*, 86–107.
[10] H. L. Xu, N. V. Tkachenko, Z. C. Wang, W. X. Chen, L. Qiao, A. Muñoz-Castro, A. I. Boldyrev, Z. M. Sun, *Nat. Commun.* **2020**, *11*, 1–8.
[11] J. M. Goicoechea, S. C. Sevov, *Organometallics* **2006**, *25*, 4530–4536.
[12] M. Waibel, F. Kraus, S. Scharfe, B. Wahl, T. F. Fässler, *Angew. Chem.* **2010**, *122*, 6761–6765; *Angew. Chem. Int. Ed.* **2010**, *49*, 6611–6615.
[13] F. S. Geitner, T. F. Fässler, *Chem. Commun.* **2017**, *53*, 12974–12977.
[14] S. Joseph, M. Hamberger, F. Mutzbauer, O. Härtl, M. Meier, N. Korber, *Angew. Chem. Int. Ed.* **2009**, *48*, 8770–8772; *Angew. Chem.* **2009**, *121*, 8926–8929.
[15] S. M. Tiefenthaler, V. Streitferdt, J. Baumann, S. Gaertner, R. M. Gschwind, N. Korber, *Z. Anorg. Allg. Chem.* **2020**, *646*, 1595–1602.
[16] W. L. Wilson, R. W. Rudolph, L. L. Lohr, R. C. Taylor, P. Pyykkö, *Inorg. Chem.* **1986**, *25*, 1535–1541.
[17] J. D. Corbett, P. A. Edwards, *J. Am. Chem. Soc.* **1977**, *99*, 3313–3317.
[18] B. Eichhorn, S. Kocak, *Zintl Ions. Struct. Bond.* (Ed.: T. Fässler), Springer, Berlin, Heidelberg, **2011**, pp. 59–89.
[19] M. Neumeier, F. Fendt, S. Gärtner, C. Koch, T. Gärtner, N. Korber, R. M. Gschwind, *Angew. Chem. Int. Ed.* **2013**, *52*, 4483–4486; *Angew. Chem.* **2013**, *125*, 4579–4582.
[20] B. Kesanli, J. Fettinger, B. Eichhorn, *Chem. Eur. J.* **2001**, *7*, 5277–5285.
[21] E. N. Esenturk, J. Fettinger, B. Eichhorn, *J. Am. Chem. Soc.* **2006**, *128*, 9178–9186.
[22] Z. M. Sun, H. Xiao, J. Li, L. S. Wang, *J. Am. Chem. Soc.* **2007**, *129*, 9560–9561.
[23] S. Scharfe, T. F. Fässler, S. Stegmaier, S. D. Hoffmann, K. Ruhland, *Chem. Eur. J.* **2008**, *14*, 4479–4483.
[24] Y. Heider, D. Scheschkewitz, *Dalton Trans.* **2018**, *47*, 7104–7112.
[25] N. E. Poitiers, L. Giarrana, K. I. Leszczyńska, V. Huch, M. Zimmer, D. Scheschkewitz, *Angew. Chem. Int. Ed.* **2020**, *59*, 8532–8536; *Angew. Chem.* **2020**, *132*, 8610–8614.
[26] C. Lorenz, F. Hastreiter, J. Hioe, N. Lokesh, S. Gärtner, N. Korber, R. M. Gschwind, *Angew. Chem. Int. Ed.* **2018**, *57*, 12956–12960; *Angew. Chem.* **2018**, *130*, 13138–13142.
[27] L. J. Schiegerl, A. J. Karttunen, J. Tillmann, S. Geier, G. Raudaschl-Sieber, M. Waibel, T. F. Fässler, *Angew. Chem. Int. Ed.* **2018**, *57*, 12950–12955; *Angew. Chem.* **2018**, *130*, 13132–13137.
[28] F. Hastreiter, C. Lorenz, J. Hioe, S. Gärtner, N. Lokesh, N. Korber, R. M. Gschwind, *Angew. Chem. Int. Ed.* **2019**, *58*, 3133–3137; *Angew. Chem.* **2019**, *131*, 3165–3169.
[29] T. Henneberger, W. Klein, T. F. Fässler, *Z. Anorg. Allg. Chem.* **2018**, *644*, 1018–1027.
[30] F. S. Kocak, D. O. Downing, P. Zavalij, Y. F. Lam, A. N. Vedernikov, B. Eichhorn, *J. Am. Chem. Soc.* **2012**, *134*, 9733–9740.
[31] J. Hertrampf, E. Schlücker, D. Gudat, R. Niewa, *Cryst. Growth Des.* **2017**, *17*, 4855–4863.
[32] T. Henneberger, W. Klein, J. V. Dums, T. F. Fässler, *Chem. Commun.* **2018**, *54*, 12381–12384.
[33] B. Kesanli, J. E. Halsig, P. Zavalij, J. C. Fettinger, Y. F. Lam, B. W. Eichhorn, *J. Am. Chem. Soc.* **2007**, *129*, 4567–4574.
[34] F. S. Geitner, M. A. Giebel, A. Pöthig, T. F. Fässler, *Molecules* **2017**, *22*, 1204.
[35] L. J. Schiegerl, F. S. Geitner, C. Fischer, W. Klein, T. F. Fässler, *Z. Anorg. Allg. Chem.* **2016**, *642*, 1419–1426.
[36] F. S. Geitner, T. F. Fässler, *Eur. J. Inorg. Chem.* **2016**, *2016*, 2688–2691.
[37] a) C. Marschner, *Eur. J. Inorg. Chem.* **1998**, *1998*, 221–226; b) H. Bürger, R. Eujen, H. C. Marsmann, *Z. Naturforsch. – Sect. B J. Chem. Sci.* **1974**, *29*, 149–152.
[38] a) C. Lorenz, F. Hastreiter, J. Hioe, N. Lokesh, S. Gärtner, N. Korber, R. M. Gschwind, *Angew. Chem. Int. Ed.* **2018**, *57*, 12956–12960; b) Y. Heider, D. Scheschkewitz, *Dalton. Trans.* **2018**, *47*, 7104–7112; see c) H. Bürger, R. Eujen, H. C. Marsmann, *Z. Naturforsch. – Sect. B J. Chem. Sci.* **1974**, *29*, 149–152.
[39] A broad peak at −7.4 ppm was detected. Due to its weak S/N this signal was not further investigated. It is located close to the signal of $[\mu\text{-}HSi_4]^{3-}$ and quite broad. This signal might constitute a similar silicide with additional coordination of $NHC^{Dipp}Cu$.
[40] So far, we could only identify H_3Si^- as degradation product of the silicides in liquid ammonia.
[41] J. Da Chai, M. Head-Gordon, *Phys. Chem. Chem. Phys.* **2008**, *10*, 6615–6620.

[42] F. Weigend, R. Ahlrichs, *Phys. Chem. Chem. Phys.* **2005**, *7*, 3297–3305.
[43] A. V. Marenich, C. J. Cramer, D. G. Truhlar, *J. Phys. Chem. B* **2009**, *113*, 6378–6396.
[44] I. G. Shenderovich, *Chem. Methods* **2021**, *1*, 61–70.
[45] I. G. Shenderovich, G. S. Denisov, *J. Chem. Phys.* **2019**, *150*, 204505.
[46] I. G. Shenderovich, *J. Chem. Phys.* **2018**, *148*, 124313.
[47] I. G. Shenderovich, *J. Chem. Phys.* **2020**, *153*, 184501.
[48] a) JB. Klein, L. Heck, *Z. Anorg. Allg. Chem.* **1975**, *416*, 269–284; b) M. J. Bezdek, S. Guo, P. J. Chirik, *Science* **2016**, *354*, 730–733.
[49] T. Kottke, D. Stalke, *J. Appl. Crystallogr.* **1993**, *26*, 615–619.
[50] H. Bürger, R. Eujen, H. C. Marsmann, *Z. Naturforsch. – Sect. B J. Chem. Sci.* **1974**, *29*, 149–152.
[51] L. Hackspill, *C. R. Hebd. Sean.Acad. Sci.* **1905**.
[52] Agilent, *CrysAlisPRO*, Agilent Technologies Ltd, Yarnton, Oxfordshire, England, **2014**.
[53] O. V. Dolomanov, L. J. Bourhis, R. J. Gildea, J. A. K. Howard, H. Puschmann, *J. Appl. Crystallogr.* **2009**, *42*, 339–341.
[54] G. M. Sheldrick, *Acta Crystallogr. Sect. A* **2015**, *71*, 3–8.
[55] G. M. Sheldrick, *Acta Crystallogr. Sect. C* **2015**, *71*, 3–8.
[56] K. Brandenburg, *Diamond Version 4.6.1*, Crystal Impact GbR, Bonn, Germany, **2019**.
[57] C. Riplinger, B. Sandhoefer, A. Hansen, F. Neese, *J. Chem. Phys.* **2013**, *139*, 134101.
[58] F. Jensen, *J. Chem. Theory Comput.* **2015**, *11*, 132–138.

Manuscript received: May 14, 2021
Revised manuscript received: June 23, 2021
Accepted manuscript online: June 29, 2021

The protonated, coinage metalated silicide $[\mathrm{NHC^{Dipp}Cu(\eta^4\text{-}Si_9)H}]^{2-}$ was detected and characterized in liquid ammonia by NMR spectroscopy, and the results were corroborated by theoretical calculations. For $[\mathrm{NHC^{Dipp}Cu(\eta^4\text{-}Si_9)H}]^{2-}$ a reduced proton hopping was identified compared to $[\mathrm{HSi_9}]^{3-}$. A new ^{29}Si-NMR signal was detected and assigned to the unprotonated cluster $[\mathrm{NHC^{Dipp}Cu(\eta^4\text{-}Si_9)}]^{3-}$. Crystals of the latter were obtained as $\mathrm{(K[2.2.2]\text{-}crypt)_2K_{0.48}Rb_{3.52}[NHC^{Dipp}Cu(\eta^4\text{-}Si_9)]_2}$.

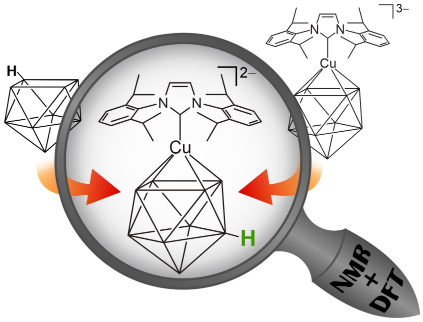

Dr. V. Streitferdt, S. M. Tiefenthaler, Dr. I. G. Shenderovich, Dr. S. Gärtner, Prof. Dr. N. Korber, Prof. Dr. R. M. Gschwind**

1 – 8

NMR-Spectroscopic Detection of an Elusive Protonated and Coinage Metalated Silicide $[\mathrm{NHC^{Dipp}Cu(\boldsymbol{\eta}^4\text{-}Si_9)H}]^{2-}$ in Solution